LBL-18720
c.2

Lawrence Berkeley Laboratory

UNIVERSITY OF CALIFORNIA

RECEIVED
LAWRENCE
BERKELEY LABORATORY

MAR 12 1985

LIBRARY AND
DOCUMENTS SECTION

Invited talk to be presented at the International Conference on Nuclear Physics, Bombay, India, December 27-31, 1984

FISSION ALONG THE MASS ASYMMETRY COORDINATE: AN EXPERIMENTAL EVALUATION OF THE CONDITIONAL SADDLE MASSES AND OF THE BUSINARO-GALLONE POINT

L.G. Moretto, M.A. McMahan, L.G. Sobotka, and G.J. Wozniak

December 1984

TWO-WEEK LOAN COPY
This is a Library Circulating Copy which may be borrowed for two weeks.

LBL-18720
c.2

Prepared for the U.S. Department of Energy under Contract DE-AC03-76SF00098

DISCLAIMER

This document was prepared as an account of work sponsored by the United States Government. While this document is believed to contain correct information, neither the United States Government nor any agency thereof, nor the Regents of the University of California, nor any of their employees, makes any warranty, express or implied, or assumes any legal responsibility for the accuracy, completeness, or usefulness of any information, apparatus, product, or process disclosed, or represents that its use would not infringe privately owned rights. Reference herein to any specific commercial product, process, or service by its trade name, trademark, manufacturer, or otherwise, does not necessarily constitute or imply its endorsement, recommendation, or favoring by the United States Government or any agency thereof, or the Regents of the University of California. The views and opinions of authors expressed herein do not necessarily state or reflect those of the United States Government or any agency thereof or the Regents of the University of California.

LBL-18720

FISSION ALONG THE MASS ASYMMETRY COORDINATE AN EXPERIMENTAL EVALUATION OF THE CONDITIONAL SADDLE MASSES AND OF THE BUSINARO-GALLONE POINT*

L.G. Moretto, M.A. McMahan, L.G. Sobotka and G.J. Wozniak

Nuclear Science Division
Lawrence Berkeley Laboratory
University of California
Berkeley, California 94720

Invited talk for the International Conference on Nuclear Physics, Bhabha Atomic Research Centre, Bombay, India, December 27-31, 1984.

*This work was supported by the Director, Office of Energy Research, Division of Nuclear Physics of the Office of High Energy and Nuclear Physics of the U.S. Department of Energy under Contract DE-AC03-76SF00098.

FISSION ALONG THE MASS ASYMMETRY COORDINATE AN EXPERIMENTAL EVALUATION OF THE CONDITIONAL SADDLE MASSES AND OF THE BUSINARO-GALLONE POINT*

L.G. Moretto, M.A. McMahan, L.G. Sobotka and G.J. Wozniak

Nuclear Science Division
Lawrence Berkeley Laboratory
University of California
Berkeley, California 94720

ABSTRACT

The importance of empirically determining the ridge line of conditional saddle points is discussed in view of the recent liquid drop model refinements, like diffuseness and finite range. Two series of experiments are presented. The first series involves the complex fragment emission from compound nuclei resulting from the ^{3}He + Ag reaction. Kinetic energy distributions and excitation functions are shown, and the conditional barriers are obtained over a range of atomic numbers. In the second series, reverse kinematic reactions like Ge, Nb, La + Be, C are studied. The fragments emitted cover the entire Z range, from Z = 1 to symmetric splitting. Their origin from a full momentum transfer intermediate is shown. From the complete charge distributions it is possible to conclude that the Businaro-Gallone transition is observed.

1. INTRODUCTION

The understanding of the fission process and the development of the liquid drop model have followed a common history. The liquid drop fission saddle point determines, in heavier systems, the boundaries of nuclear stability and the dominance of symmetric splitting, while, in

*This work was supported by the Director, Office of Energy Research, Division of Nuclear Physics of the Office of High Energy and Nuclear Physics of the U.S. Department of Energy under Contract DE-AC03-76SF00098.

lighter systems, with the loss of stability of the mass asymmetry degree of freedom, it determines the disappearance of fission as a process separate from evaporation.

In a way, the mass asymmetry degree of freedom appears to be the most interesting normal mode at the saddle point. As mentioned above, its ever increasing stability above the Businaro-Gallone point defines fission as a separate process, whose mass distribution progressively sharpens as one moves toward the upper end of the periodic table. Below the Businaro Gallone point, the mass asymmetry mode loses stability; thus the associated fission mass distribution should portray a minimum at symmetry and should connect monotonically with the mass distribution arising from evaporation.

An experimental study of the mass asymmetry degree of freedom must rely on the measurement of the exit channel mass/charge distribution which, unfortunately, is a characteristic property of the scission point, rather than of the saddle point. Such a difficulty is mitigated by the fact that, for lighter nuclei, saddle and scission points are almost degenerate, so that little or no evolution can be expected from saddle to scission point. For heavier nuclei, saddle and scission points may be quite far apart for symmetric splitting, so that the observed mass distribution results from a combination of the initial asymmetry distribution at the saddle, and of the dynamical evolution from saddle to scission. Yet, even for the heavier systems, there is a range of mass asymmetries, near the most asymmetric limit, where the saddle point and the scission point are, in fact, nearly degenerate.

These general ideas have formed the basis of a theoretical paper that discusses in a unified way the compound nucleus emission of fragments with masses ranging from protons or neutrons to one half that of the compound nucleus.[1] The key concepts in this development are the "conditional" saddle points at fixed mass asymmetry and their locus called "ridge line" in analogy to "saddle point."

Experimentally, information has been limited to the measurement of the fission barriers of heavy nuclei.[2] These data were

instrumental in removing the ambiguity arising from the Coulomb term and the surface term in the liquid drop model.[3] From the experimental barriers shell effects were obtained for both ground state and saddle point.

Similar information could be obtained by performing measurements of the conditional barriers as a function of mass asymmetry. This has been prevented so far by the very small decay rates that one encounters for lighter systems. Recently, however, we have been able to overcome some of the difficulties associated with the relevant experiments. Two classes of experiments will be reported here. The first deals with the emission of complex fragments from compound nuclei[4] and their excitation functions leading to the determination of the associated conditional barriers. The second is the measurement of the entire charge distribution from alpha particles to symmetric fragments and the verification of the Businaro-Gallone transition.[5]

2. COMPOUND NUCLEUS EMISSION OF COMPLEX FRAGMENTS AND THEIR EXCITATION FUNCTIONS

Complex fragments have been observed in high-energy proton reactions.[6-9] However, the origin of these fragments cannot be easily or unequivocally traced to a well-characterized compound nucleus because precompound processes dominate and multiple fragmentation of the target is possible. Heavy-ion reactions at low bombarding energies[10] have been shown to produce equilibrated compound nuclei (e.g., ^{26}Al) from which Li or Be nuclei are emitted with low probability. At bombarding energies above ~8 MeV/nucleon,[11] however, the fragments of interest are also produced by projectile breakup, thus complicating the study of the compound nucleus decay.

We have obtained experimental evidence for the emission of complex nuclei from helium through fluorine by compound nuclei produced in the reaction 90 MeV ^{3}He + ^{nat}Ag.[4] The specific choice of ^{3}He as projectile was dictated by two reasons. On one hand it is desirable to have a relatively low velocity projectile in order to minimize preequilibrium losses, but massive enough to bring in sufficient energy. On the other, the mass of the projectile should

be sufficiently smaller than those of the complex fragments of interest in order to rule out the ambiguity of projectile fragmentation or multinucleon transfer.

The ^{3}He beam was produced by the Lawrence Berkeley Laboratory 88-Inch Cyclotron. The atomic number and the energy spectra of the intermediate mass fragments were measured in a set of three standard gas, solid-state (300 μm, $d\Omega \sim 1.2$ msr) ΔE-E telescopes operated at a pressure of 100 torr. Alpha particles were detected in a separate solid-state telescope (40 μm, 5 mm, $d\Omega = 0.35$ msr). Angular distributions were obtained from 20° to 170° in the laboratory.

In order to determine the existence of an isotropically emitting source and its velocity, the laboratory energy spectra were transformed into invariant cross-section plots in velocity space which are presented in Fig. 1. The peak cross section for a heavy complex fragment, such as carbon, has a constant value and occurs at the same c.m. velocity from 170° to 40° (as indicated by the position of the X's relative to the circular arc). At the most forward angle the peak cross section occurs at a slightly increased velocity. Similarly, the higher velocity region (the region near the arc with the larger radius) shows no significant change in the backward hemisphere, but does stretch out at forward angles. For a light complex fragment such as Li, the peak of the cross section occurs at a constant c.m. velocity for a smaller backward angle region (170° to 120°). Forward of 120° the peak increases both in cross section and in velocity. The slope of the high-energy tail does not change significantly for the three most backward angles, but the intensity of the tail increases as the scattering angle decreases. The ^{9}Be and B fragments show a behavior intermediate between that of Li and C. In general, the heavier ejectiles show patterns more consistent with the emission from a single source.

Two conclusions can be drawn from these invariant cross-section plots. First, for all elements there is an angular region in the backward hemisphere where only a single component is observed, which can be characterized by the c.m. emission. This angular region

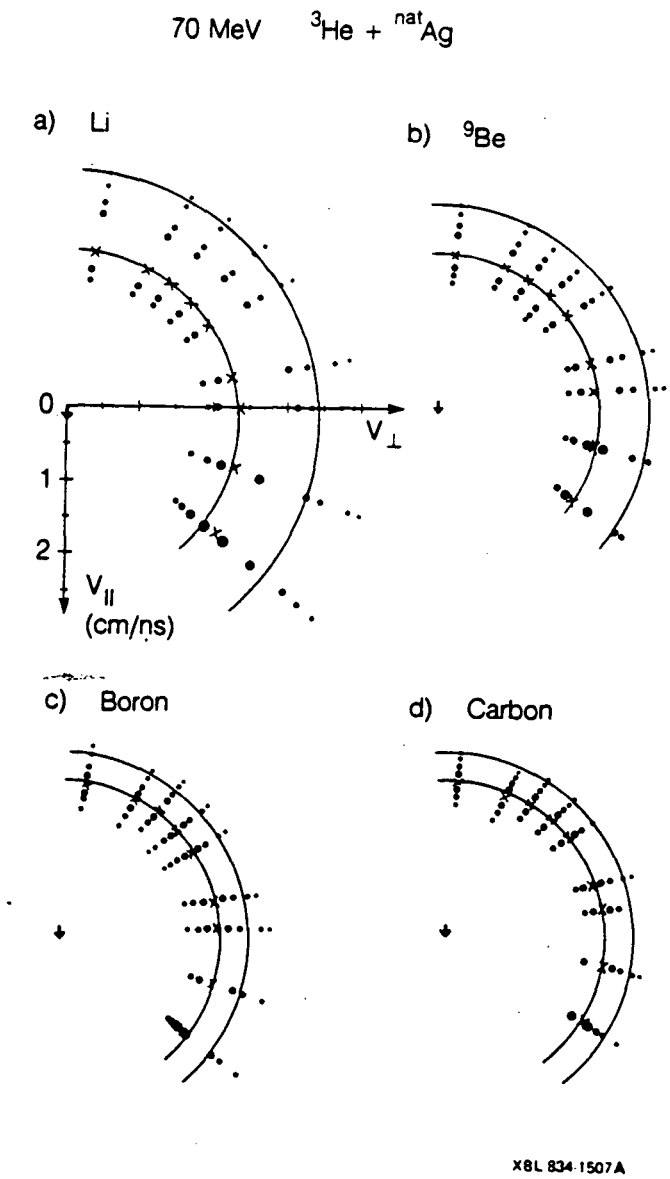

Fig. 1. Invariant cross section plots $\left(\propto \frac{1}{V^2}\frac{d^2\sigma}{d\ dV}\right)$ for representative ejectiles (Li, ^{9}Be, B, and C). The diameter of the dots is proportional to the logarithm of the cross section and the X's indicate the peak of velocity distribution. The two large arcs are sections of circles centered on the c.m. velocity (center arrow) appropriate for complete fusion. The beam direction (0°) is indicated by the c.m. velocity vector.

increases and extends to more forward angles as the ejectile mass increases. Second, there is a component of non-c.m. emissions that results in harder energy (or velocity) spectra at forward angles.

The energy spectra of the equilibrium component in the c.m. system are shown in Fig. 2. The mean energies of the spectra are Coulomb-like and increase as the charge of the fragment increases. The most interesting feature in the energy spectra of the equilibrium component is the evolution from a Maxwellian shape for α-particles (not shown) or Li ions through a more symmetric shape for B or C to a symmetric shape for the heaviest ejectiles, as predicted in Ref. 1. In previous high energy proton studies,[8-9] an exponential tail was observed for all ejectiles. This tail, produced by sources other than equilibrium emission from the center-of-mass system, masks the shape of the equilibrium component. At forward angles, our data also show the presence of a nonequilibrium exponential tail.

The experimental yields of the equilibrium component are shown in Fig. 3. To minimize contributions from sources other than the compound nucleus, we have plotted the yields only for the most backward angle (171°). These yields drop precipitously in going from Z = 2 to Z = 3, after which they decrease more slowly. The one exception is the enhanced Z = 6 yield.

The yield from an equilibrium statistical emission process should be roughly proportional to a factor $\exp[-B_Z/T_Z]$, where B_Z is the emission barrier for fragment Z and T_Z is the temperature at the barrier. More quantitatively, the decay width is given by

$$\Gamma_Z \propto T_Z[E/(E - B_Z)]^2 \exp[2\sqrt{a(E - B_Z)} - 2\sqrt{aE}] \tag{1}$$

$$\tilde{\propto} \exp[-B_Z/T_Z] \quad . \tag{2}$$

To calculate the theoretical yields, the following expression for the barrier was used

$$B_Z = U_1 + U_2 + \frac{Z_1 Z_2 e^2}{d} + U_{prox} - U_{CN} \quad , \tag{3}$$

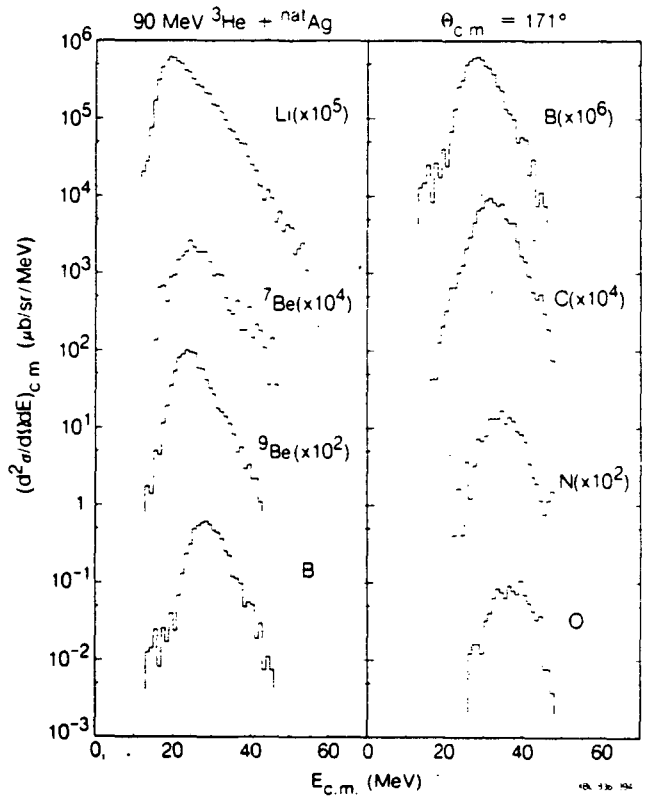

Fig. 2. Energy spectra in the c.m. system for various ejectiles detected at $\Theta_{c.m.}$ = 171°. Before correction for carbon contamination the lower level threshold varied from 4 to 12 MeV in the c.m. for Li to O ejectiles, respectively.

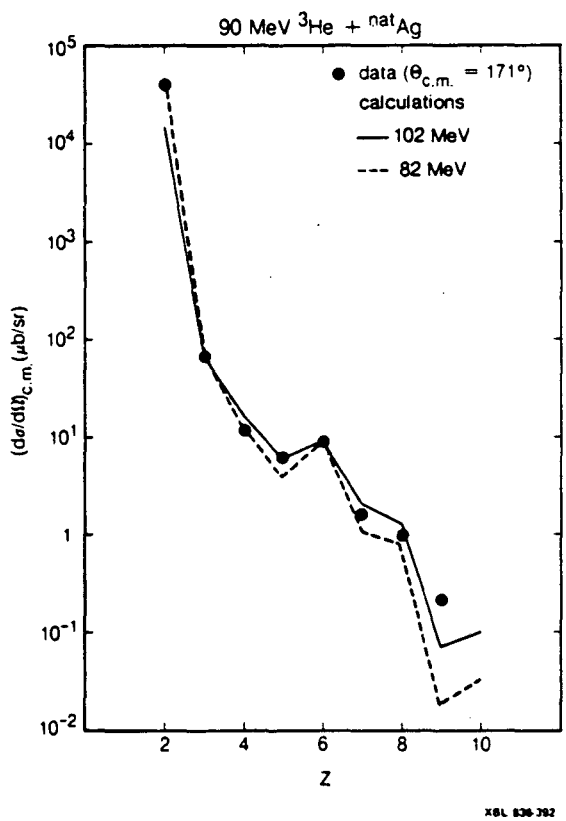

Fig. 3. Experimental (circles) and theoretical yields versus ejectile atomic number (Z).

where U_1 is the experimental mass of the light fragment, U_2,U_{CN} are the droplet model masses of the residual and compound nucleus, respectively, and U_{prox} is the proximity potential. The center-to-center distance d in the interfragment Coulomb term was taken to be $d = 1.225(A_1^{1/3} + A_2^{1/3}) + 2$ fm. The addition of 2 fm was done to obtain rough agreement with the energy spectra. The temperature (T_z) was evaluated using $E - B_z = aT_z^2$. A compound nucleus excitation energy (E) of 102 MeV (the value for full momentum transfer) and a level density parameter (a) of A/8 were assumed. The calculated yields (Eq. 1) for each isotope were multiplied by 2I + 1 (where I is the ground state spin of the light fragment) and then summed. The theoretical ejectile yields were calculated as a ratio Γ_z/Γ_6 and have been normalized to the data at Z = 6 in Fig. 3.

The agreement between the data (circles) and this simple equilibrium statistical calculation (solid line) is exceptionally good for Z = 3-9. The calculation underpredicts the α-particle yield because it only takes into account first chance emission, whereas substantial amounts of higher chance α-emission occur. Precompound emission is expected to leave the compound nucleus with a broad excitation energy distribution with a most probable value of ~85 MeV. A calculation (not shown) with this lower excitation energy also reproduces the relative yields of the heavy fragments quite well but overpredicts the yield of first chance α-emission. More detailed comparisons between the data and theory require calculations that include precompound emission; however, the substantial agreement depicted in Fig. 3 does indicate that an equilibrated process is responsible for the emission of these complex fragments.

Complete excitation functions obtained from the $^3He + {}^{nat}Ag$ measurements are shown in Fig. 4 for a series of decay products. The measurements were restricted to the backward angles (120° - 160°) in order to insure measurement of only the equilibrium component. The total cross sections were obtained by integrating over angle using the angular distribution formula of Moretto.[1)]

With increasing bombarding energy, the cross sections (see Fig.

4) rise rapidly and then flatten at higher energies. This is a characteristic signature of compound nucleus emission, and reinforces the assignment of compound nucleus decay that was made previously on the basis of data obtained at 90 MeV. The cross section for Z = 3 is a factor of 1000 lower than that for Z = 2, and for the heavier fragments it is even lower. In spite of these low cross sections, we were able to measure an excitation function over 2-3 orders of magnitude up to Z = 11, with a detection limit of about 50 nb.

The experimental excitation function data have been fitted using a transition state formalism, analogous to that used to fit fission excitation functions.[1] As shown in Ref. 1, the decay width for first-chance emission of a fragment of charge Z can be written as

$$\Gamma_Z = \frac{1}{2\pi\rho(E)} \int_0^{E-B_Z} \rho_Z^*(E - B_Z - \varepsilon)d\varepsilon \tag{4}$$

where $\rho(E)$ is the compound nucleus level density, B_Z is the conditional barrier height, and $\rho_Z^*(E - B_Z - \varepsilon)$ is the level density at the conditional saddle with a kinetic energy ε in the decay mode. The neutron width Γ_n can be written as

$$\Gamma_n = \frac{2mR^2 g}{2\pi\rho(E)} \int_0^{E-B_n} \varepsilon\rho(E - B_n - \varepsilon)d\varepsilon \tag{5}$$

We make the assumption that the ratio of the decay widths, Γ_Z/Γ_n, is proportional to the ratio of the cross section for complex fragment emission, σ_Z, to that for complete fusion, σ_f, i.e.,

$$\Gamma_Z/\Gamma_n \simeq \frac{\Gamma_Z}{\Gamma_t} \simeq \frac{\sigma_Z}{\sigma_t} \simeq \frac{\sigma_Z}{\sigma_R} \tag{6}$$

This is reasonable in this mass region because $\Gamma_n \gg \sum_{Z\geq 1}^{\infty} \Gamma_Z$. One can then calculate $\Gamma_Z/\Gamma_n(E)$ using an appropriate choice for the level density expressions. A Fermi gas level density was used because

it gives an analytical expression for Γ_f/Γ_n. A simple angular momentum dependence has been included by adding to the barriers the rotational energies appropriate to the ground and saddle point deformations.

Using the above expression for Γ_z/Γ_n, the barriers B_z, and the ratio a_z/a_n, of the level density parameters were extracted from fits to the experimental data σ_z/σ_R. These fits are shown by the solid lines in Fig. 4. The agreement between the data and the fits is remarkably good for all Z-values and confirms that these products originate from compound nuclear decay.

The barriers and values of a_z/a_n extracted from the fits are shown by the circles in Fig. 5 as a function of Z/Z_{CN}. The extracted barriers increase dramatically as the exit channel becomes more symmetric. Some evidence of shell effects in the exit channel is visible in the barrier for carbon emission, Z = 6, which is lower than those of the neighboring elements. The values of a_z/a_n extracted from the fits tend to oscillate in the range of 0.98-1.02, or 1.07-1.12 if preequilibrium emission is included. The values of a_f/a_n obtained in fitting fission excitation functions have been shown to reflect shell effects in the saddle point configuration.[2)] One might hope in the future to relate the variation of a_z/a_n with exit channel charge and mass to saddle point shell effects. Future measurements of A as well as Z should give detailed information on saddle point shell effects.

The extracted barriers and level density parameters are subject to several uncertainties due to the assumptions made in this simple analysis. Not included in the fits are the effects of preequilibrium emission on the initial excitation energy. This can be estimated using the geometry dependent hybrid model from the statistical code ALICE[12] to calculate the excitation energy distribution after the fast precompound stage. Preequilibrium emission is negligible at the lowest bombarding energies, but significantly reduces the average excitation energy of the compound nucleus at bombarding energies of 90 and 130 MeV. However, when at each bombarding energy, the calculated excitation energy distribution after precompound emission was used to

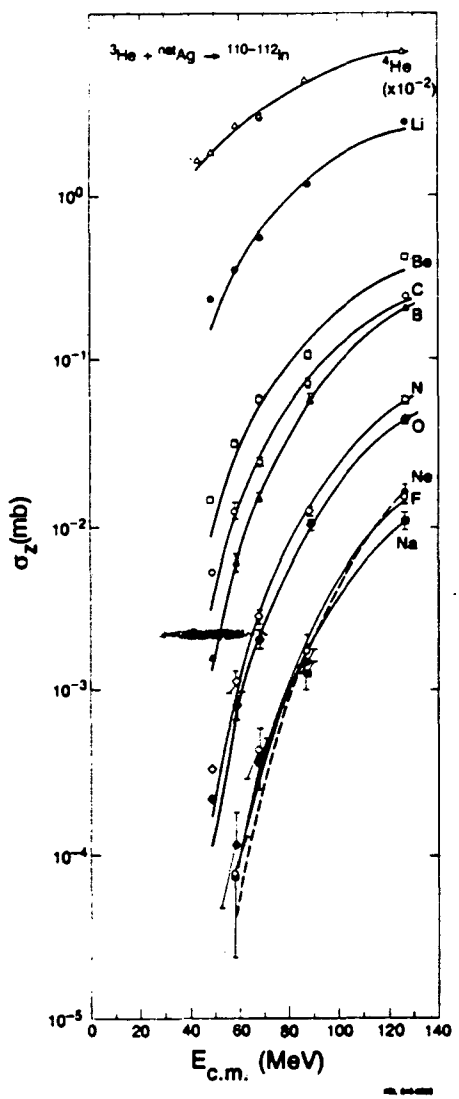

Fig. 4. Dependence of the total integrated cross sections for emission of complex fragments on the center-of-mass energy, $E_{c.m.}$ in the reaction ^{3}He + ^{nat}Ag. The points and error bars correspond to the experimental cross sections. The curves are fits with the parameters of Fig. 5.

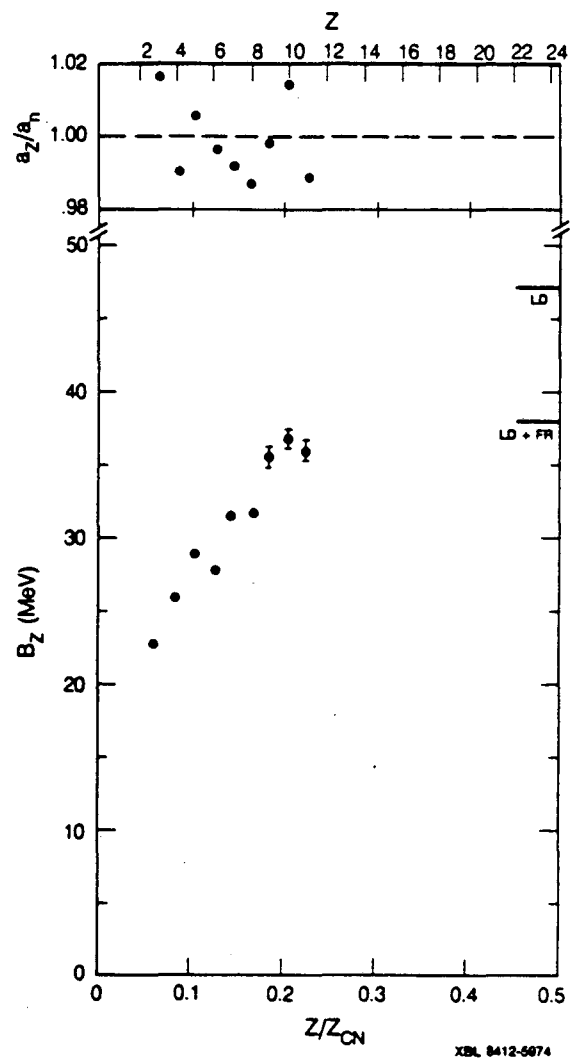

Fig. 5. The emission barriers, B_Z, and ratio of level density parameters, a_Z/a_n, extracted in fitting the excitation functions as a function of asymmetry, Z/Z_{CN}. (Z/Z_{CN} = 0.5 corresponds to symmetric splitting.) The points are the extracted parameters, excluding pre-equilibrium emission.

fit the data, the values of the barriers are lowered only slightly, less than 1 MeV, and the values of a_z/a_n are raised by ~7%. This is understandable since the barriers are most sensitive to the steep part of the excitation function at lower energies and a_z/a_n is sensitive to the curvature at higher energies. First-chance emission from a fully equilibrated system was assumed, with the fusion cross section $\sigma_f(\ell)$ given by the sharp cutoff model with $\ell_{crit} = 16$, as given by by the Bass Model.[13] This assumption should be valid for Z > 2, but is clearly invalid for Z = 2. Thus in the following discussion, the fitted parameters for Z = 2 are ignored. The sensitivity of the fit to the various input parameters has also been examined. Varying each of these parameters within reasonable limits makes a difference in the extracted barriers and values of a_z/a_n, of at most 5% for all values of Z. In addition, the formalism was tested for "fission" by fitting fission excitation functions. The values of the fission barriers and a_f/a_n extracted with our fitting procedure agree quite well with values quoted in the literature.[2] This agreement indicates that our simple formalism gives a reasonable approximation to more sophisticated codes.

The sensitivity tests described above show that the extracted emission barriers have an uncertainty of ~2 MeV. These results are ideal for testing the finite-range correction to the liquid drop model.

3. COMPLETE CHARGE DISTRIBUTIONS AND THE ROLE OF THE BUSINARO-GALLONE POINT

The sharp distinction between evaporation and fission in relatively heavy compound nuclei is a result of a specific topological feature of the liquid drop model potential energy surface V(Z) as a function of mass asymmetry Z. This feature is a deep minimum at symmetry (fission region) flanked at greater asymmetries by the Businaro-Gallone mountains which in turn descend at even larger asymmetries ("evaporation" region). The corresponding mass distribution from compound nucleus decay is approximately proportional to $\exp[-V(Z)/T_Z]$ and shows a peak at symmetry (fission peak) and two wings at the extreme asymmetries (evaporation wings). The qualitative

dependence of the potential energy and of the mass yield vs. asymmetry is shown in Fig. 6a for a heavy nucleus.

With decreasing total mass the potential energy surface undergoes a topological change when the fissility parameter x crosses the so-called Businaro-Gallone point.[14] At this point (x_{BG} = 0.396 for ℓ = 0 and decreases for larger ℓ values) the second derivative of the potential energy with respect to the mass asymmetry coordinate evaluated at symmetry vanishes.[1,14,15] Thus below the Businaro-Gallone point there is no longer a traditional fission saddle point, and the monotonically increasing potential energy towards symmetry implies the disappearance of fission as a process distinct from evaporation. Thus the mass distribution should show the two evaporation wings extending as far as symmetry where a minimum should be observed. This is illustrated in Fig. 6b.

Such a transition has never been observed, as it requires the measurement of the entire mass distribution from symmetry to the extreme asymmetry of α,p evaporation for a series of systems straddling the Businaro-Gallone point. This measurement is made very difficult by the low yield for symmetric decay of the compound nucleus in this general mass region, and by the need to verify that the fragments were produced by a compound nucleus mechanism.[4]

We have measured complete charge distributions from protons to symmetric splitting for a variety of nuclei and we have observed the Businaro-Gallone transition. Such a transition is inferred from the disappearance of the fission peak in the mass yield as the compound nucleus mass was decreased from ^{148}Eu, ^{102}Rh to ^{83}Kr.

The use of reverse kinematics (projectile heavier than the target) was crucial in performing these measurements. This technique virtually eliminates the problems associated with low cross section measurements due to the presence of light element target contaminants. Furthermore, reverse kinematics provides a large center-of-mass (c.m.) velocity which facilitates the verification of full momentum transfer and allows for easy identification of the fragment's atomic number at the higher lab energies. Finally the high energy solution at forward angles corresponds to very backward angles

in ordinary kinematics. This enhances the observation of compound nucleus decay and virtually eliminates any possible deep-inelastic contamination.

The experiments were carried out at the Lawrence Berkeley Laboratory SuperHILAC utilizing beams of 550-Mev ^{74}Ge, 782-MeV ^{93}Nb and 1157-MeV ^{139}La, to bombard targets of 0.54 mg/cm^2 ^{12}C and 1.0 mg/cm^2 ^{9}Be. The detection system consisted of four solid state ΔE - E silicon telescopes (40-70 μm, 3-5 mm) situated at 7.5°, 15°, 25° and 35° from the beam with solid angles of approximately 1.0 msr. For the heavier ^{139}La beam these detectors were supplemented by two gas ΔE-solid state E telescopes at -7.5° and 22.5°.

The observed laboratory energies represent only the higher energy kinematic solution. In general, the lower solution is not observed because of the energy threshold due to the thickness of our ΔE detectors. Thus the laboratory energy of the upper solution, the measured atomic number (Z), and angle permitted us to verify that the recorded events both originated from a system with full momentum transfer and had a c.m. energy independent of angle. This is shown for two representative elements in Fig. 7.

The mean laboratory energies for each Z-value were converted to velocities with two different assumptions for the relationship between the Z and the mass of the detected fragments. These velocities are then decomposed into two components. One component, along the beam direction, is assigned an arbitrary value; the other component is that required to reconstitute the original velocity. (For convenience this second component is shown as the c.m. energy in Fig. 7.) In this way, for each laboratory angle we can draw a curve representing the dependence of the c.m. energy upon the source velocity. This procedure is followed for each angle that is smaller than the kinematically allowed maximum angle. The intersection of these lines determines, in a model independent way, both the momentum transfer and the energy in the center of mass. The error bars shown on the lines in Fig. 7 reflect the uncertainty in the mean laboratory energies.

The results from this type of analysis for the ^{93}Nb + ^{12}C

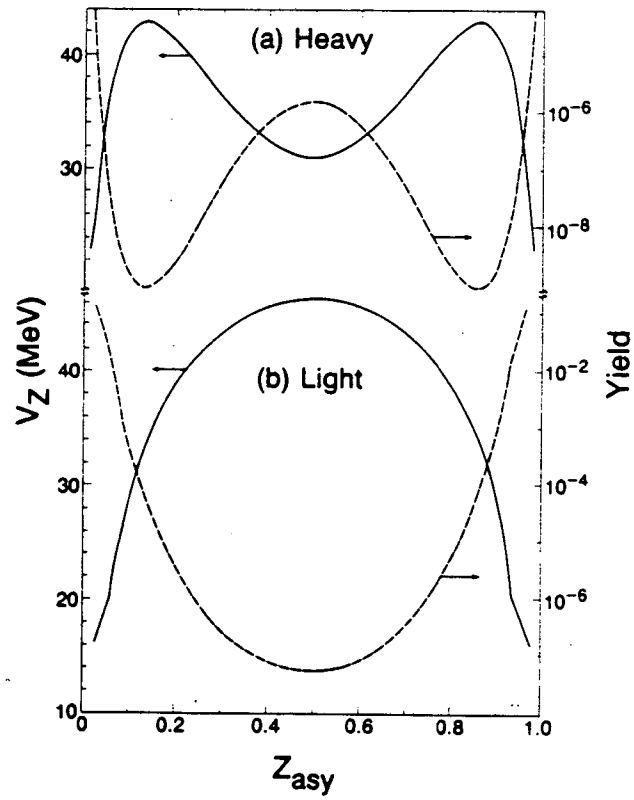

Fig. 6. Comparison of the potential energy surfaces (solid curve) and expected yields (dashed curve) for a) a heavy CN (Au at $\ell = 0$ and $E^* = 97$ MeV) and b) a light CN (Ge at $\ell = 0$ and $E^* = 72$ MeV).

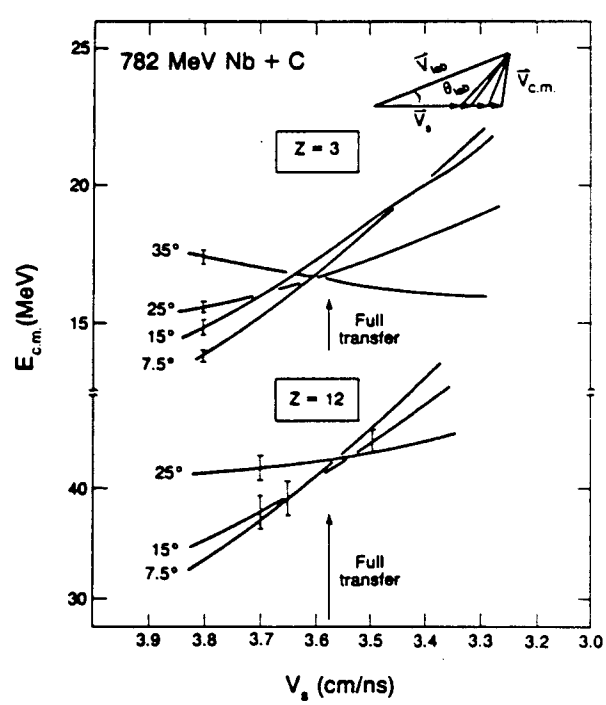

Fig. 7. The line for each angle gives the locus of solutions for both $E_{c.m.}$ and V_S. The intersection of the various lines fixes these quantities. The velocity corresponding to complete linear momentum transfer is indicated. This figure was drawn assuming that the masses follow the line of β-stability.

system are shown in Fig. 8. The upper part of this figure demonstrates that with either mass assumption all of the measured products result from the decay of a system with full momentum transfer. For the other systems studied, the extracted source velocities are also independent of Z within a few percent of the velocity expected for full momentum transfer. The deduced c.m. energies are shown in the lower portion of Fig. 8. These energies are reproduced by a Coulomb calculation for two spheres with a surface separation of 2 fm. This same separation also reproduces the c.m. energies from the ^{74}Ge induced reactions; however a larger separation is required for the ^{139}La data. Both the full momentum transfer and the invariance with angle of the c.m. energies seen above are consistent with compound nucleus decay.

The experimental cross sections for 530-MeV ^{74}Ge, 782-MeV ^{93}Nb and 1157-MeV ^{139}La + ^{9}Be systems are shown in Fig. 9. The cross sections are plotted as a function of charge asymmetry ($Z_{asy} = Z_{detected}/Z_{total}$). The lack of enhancement in yield near the target Z supports the compound nucleus origin of the products rather than a deep-inelastic origin. The yield from the ^{74}Ge + ^{9}Be system, with a fissility parameter of x = 0.31, decreases steadily as one moves towards symmetry. The yields from the ^{93}Nb + ^{9}Be system (x = 0.40) are essentially constant from Z_{asy} = 0.2 to 0.4 while the yields from the ^{139}La + ^{9}Be system (x = 0.50) show the characteristic fission peak at symmetry. These three systems clearly exhibit the qualitative trends expected from the topological changes in the potential energy surface predicted by the liquid drop model (see Fig. 6).

A quantitative comparison between these data and a compound nucleus calculation based upon the liquid drop model is also shown in Fig. 9. The absolute yields were calculated from the expression

$$\sigma_Z = \pi \lambda^2 \sum_{\ell=0}^{\ell_m} (2\ell + 1) \frac{\Gamma_Z(\ell)}{\Gamma_n + \Gamma_p + \Gamma_\alpha} \tag{7}$$

where $\frac{\Gamma_z}{\Gamma_n}$ is given by Eq. (1).

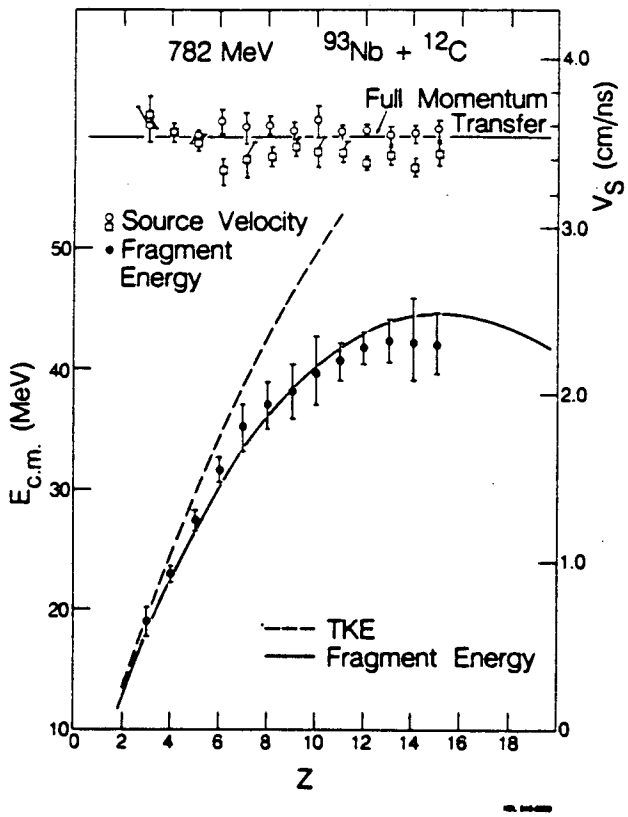

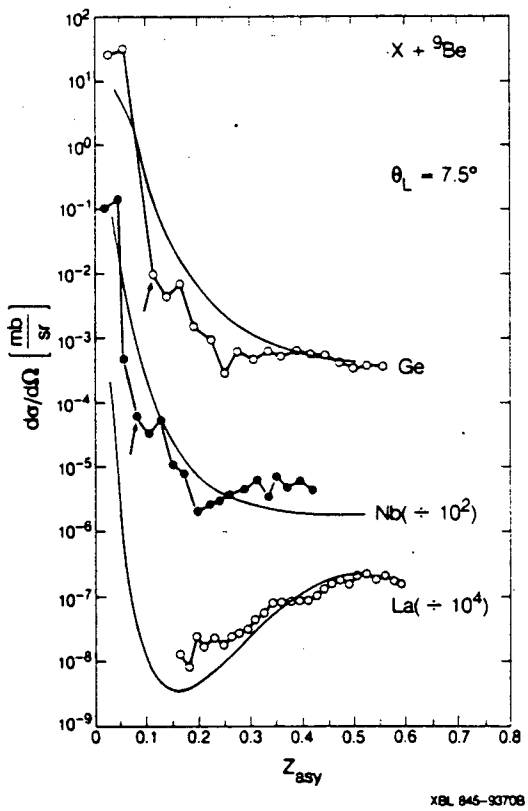

Fig. 8. The deduced c.m. energies (filled circles) and source velocities (open symbols) for the ^{93}Nb + ^{12}C system. Source velocities were determined assuming that the product mass followed the line of β-stability (open circles) or the charge equilibration line (open squares). A Coulomb calculation for two spheres is shown both for the c.m. energy of the light fragment (solid line) and the total kinetic energy (dashed line). The value of the source velocity expected for full momentum transfer is indicated by the horizontal line. The error bars indicate the uncertainty of the intersection point shown in Fig. 7.

Fig. 9. Center-of-mass cross sections for products from the ^{74}Ge, ^{93}Nb and ^{139}La + ^{9}Be systems detected at θ_{Lab} = 7.5°. The solid line is a liquid drop model calculation of the fragment yield at $\theta_{c.m.}$ = 30°. The arrows indicate the entrance channel asymmetry. See text. Data below z_{asy} = 0.15 were not obtained for the La + Be system, due to a limited dynamic range of the telescope.

The angular distribution expressions given in Ref. 1 were employed to calculate the differential cross section ($d\sigma/d\Omega$). The c.m. angles of the data in Fig. 9 vary as a function of Z. However, the average c.m. angle is approximately 30°, so this angle was chosen for comparison. The agreement in absolute magnitude and in trend between this calculation and the data confirms the compound nuclear origin of these fragments.

In summary, we have shown that fragments with atomic numbers covering the entire range of the mass asymmetry coordinate are produced from the decay of an excited compound nucleus. The observed Z distributions indicate that the topological transition expected at the Businaro-Gallone point does indeed take place in the region of $A \sim 100$. The exact position of the Businaro-Gallone point and its angular momentum dependence can in principle be established by a systematic study of the Z or A distributions as the fissility parameter x and the rotational parameter y are varied.

This work was supported by the Director, Office of Energy Research, Division of Nuclear Physics of the Office of High Energy and Nuclear Physics of the U.S. Department of Energy under Contract DE-AC03-76SF00098.

4. REFERENCES

1. Moretto, L.G., Nucl. Phys. A247, 211 (1975).
2. Moretto, L.G., in "Physics and Chemistry of Fission," Rochester, N.Y., 1973, pg 329.
3. Myers, W.D., "Droplet Model of Atomic Nuclei," IFI/Plenum Data Company, N.Y., 1977.
4. Sobotka, L.G., Padgett, M.A., Wozniak, G.J., Guarino, G., Pacheco, A.J., Moretto, L.G., Chan, Y., Stokstad, R.G., Tserruya, I. and Wald, S., Phys. Rev. Lett. 51, 2187 (1983).
5. Sobotka, L.G., McMahan, M.A., McDonald, R.J., Signarbieux, C., Wozniak, G.J., Padgett, M.L., Gu, J.H., Liu, Z.H., Yao Z.O. and L.G. Moretto, Phys. Rev. Lett.
6. Baker, E. et al., Phys. Rev. 112, 1319 (1958).
7. Dostrovsky, I. et al., Phys. Rev. 118, 781 (1960).
8. Westfall, G.D. et al., Phys. Rev. C17, 1368 (1978).
9. Green, R. and Korteling, R., Phys. Rev. C22, 1594 (1980).

10. Hanson, D.L. al., Phys. Rev. C9, 929 (1974).

11. Stokstad, R.G. et al., Phys. Rev. C16, 2249 (1977).

12. Blann, M., Lawrence Livermore National Laboratory Report UCID-20169 (1984).

13. Bass, R., Nucl. Phys. A231, 45 (1974).

14. Businaro, U.L. and Gallone, S., Nuovo Cim. 1, 629, 1277 (1955).

15. Nix, J.R., Nucl. Phys. A130, 241 (1969) and references therein.

This report was done with support from the Department of Energy. Any conclusions or opinions expressed in this report represent solely those of the author(s) and not necessarily those of The Regents of the University of California, the Lawrence Berkeley Laboratory or the Department of Energy.

Reference to a company or product name does not imply approval or recommendation of the product by the University of California or the U.S. Department of Energy to the exclusion of others that may be suitable.

TECHNICAL INFORMATION DEPARTMENT
LAWRENCE BERKELEY LABORATORY
UNIVERSITY OF CALIFORNIA
BERKELEY, CALIFORNIA 94720